minerals

MDPI

Article

Experimental Development of Transport Percussion Marks on Obsidian Clasts, Pilauco Site, Chilean Northwestern Patagonia

Catalina Madrigal [1], Haroldo Lledó [1], Daniel Fritte [2,3] and Mario Pino [2,3,*]

1 Carrera de Geología, Departamento de Obras Civiles y Geología, Universidad Católica de Temuco, Temuco 4781312, Chile; catalina.madrigal.geo@gmail.com (C.M.); hlledo@uct.cl (H.Ll.)
2 Instituto de Ciencias de la Tierra, TAQUACH, Laboratorio Natural Pilauco, Facultad de Ciencias, Universidad Austral de Chile, Valdivia 5090000, Chile; daniel.fritte@uach.cl
3 Foundation for Heritage Pleistocene Studies at Osorno (FEPPO), Osorno 5290000, Chile
* Correspondence: sitios.pilauco.los.notros@gmail.com; Tel.: +56-997418947

Abstract: In the Pilauco site (40°34′11″ S, 73°06′17″ W; 13,570 ± 70–12,540 ± 90 14C year BP), a previous geochemical trace analysis suggested that the Puyehue-Cordón Caulle Volcanic Complex is the most likely source for obsidian and dacitic glass artifacts at Pilauco. It was hypothesized that the glassy rocks were probably collected from a pebble beach deposit, as deduced by the presence of crescentic percussion marks on the artefact cortexes. An experimental study was designed using pebble obsidian clasts. Bidirectional transport produced by the waves on a beach was imitated by an oscillating table, using time lapses equivalent to a transport of 0.7 to 20 km. One hundred clasts were randomly selected and marked. The morphological changes were registered, measured and photographed after seven sequential runs. At the end of the experiment at 20 km, the mass loss of rounded and fractured clasts was 5% and 11%, respectively. Crescent, circular, pseudo-circular and irregular percussion marks occurred in both types of clasts. In all cases, the crescent marks developed a pseudo-frosted surface appearance, giving a whiter tone that masks the black color of the obsidian, exactly as observed in the cortex of the artifacts knapped in dacitic glass at the Pilauco site. Thus, it is highly probable that the vitreous material was obtained from a beach sourced by the Puyehue-Cordón Caulle Volcanic Complex.

Keywords: volcanic glass; archaeology; transport; surficial marks; Pilauco; Chile

1. Introduction

The Pilauco paleontological and archaeological site is located in the Central Depression of northwestern Chilean Patagonia, west of the Andes Mountains, in the city of Osorno, Región de los Lagos (40°34′ S–73°07′ W; Figure 1). It is one of the most important and oldest Late Pleistocene sites in Chile [1–6]. The richness of its findings has made it possible to reconstruct part of the life of the first inhabitants of northwestern Chilean Patagonia during that time, as well as the associated existing and extinct flora and fauna [7]. The research conducted at the Pilauco site has been approached from several disciplines, i.e., geology, paleontology, paleobotany, archaeology and astrophysics, with a transdisciplinary strategy [8–12].

During the Late Pleistocene, the human settlement of South America through the Bering Strait became one of the most inspiring research issues for archaeology ([1,2] and references therein). South American archaeology has strongly focused on understanding the relationship between early Americans and their natural environment [3–6,9,13–15]. The study of lithic artifacts has often been carried out by combining morphotechnological studies with geochemical identification of raw material sources (e.g., [16–18]). In this continent, the nature of the lithic assemblages is diverse and records the coexistence of unifacial and bifacial technologies [19]. In general, the lithic artifacts described are usually

unifacial and quite simple, as is the case of the Pilauco site [20]. Characteristics of the artifact surface crust fabric are barely mentioned [9].

Figure 1. Location map of Pilauco site (red dot) in Osorno City. A green dot indicates the source of the obsidian in the north of Chile. Image obtained from Google Earth.

2. Geological Setting

Natural processes can also occasionally produce pseudo-artifacts, producing pieces similar to an artifact both in raw material, size and shape [21]. One of the methods applied to solve this problem is to obtain the geochemical fingerprint of primary or secondary raw material sources from outside the site, to rule out the possible contribution of nature [22]. In the almost complete absence of flint, many of the carving materials used in South America, such as aphanitic volcanic rocks, are distributed over large regions. Thus, it is difficult to identify precise sources in the territories. On the other hand, one of the most used materials in South America is obsidian. These rocks have very good carving properties, and their outcrops are restricted to a few volcanoes. In them, the geochemical fingerprint is so characteristic that it allows to identify the artifacts that were knapped with each type of obsidian [18,23–26].

In the context of Pilauco, geochemical studies of a set of artifacts and chips composed of rhyodacitic and dacitic glass made it possible to propose that the source of these raw materials corresponds to a volcanic complex located about 80 km east of the site [9]. Frequently, surface micro-texture analyses use scanning electron microscopy of the sandy fraction of quartz grains ([27] and references therein). Crescentic or semilunar percussion marks found on quartzite or chert pebbles were interpreted as high-velocity impacts [28]. Additionally, in the Upper Ganges basin, under high kinetic energy, all quartzite pebbles exhibited semilunar percussion scars [29]. Similarly, the surfaces of boulders and pebbles from the Upper Triassic of New Brunswick, Canada, are characterized by the same marks. In this case, they were interpreted to have been formed by percussion between clasts during fluvial transport [30]. Additionally, using carbon casts, an electron microscopic study of pebble surface marks was published [31]. They used samples obtained from beaches, glacial and fluvial environments and described an extensive collection of microfractures. Semilunar percussion marks in sand- and gravel-sized grains occur because of strong collisions between clasts [28]. They resemble part of a conchoidal fracture without forming a complete fracture plane, which would occur with large amounts of energy. However, at Pilauco, it was not possible to resolve the origin of the surface percussion marks visible on the cortex of some of the knapped pieces [9]. It is remarkable that the almost black color of the dacitic glass and obsidian artifacts is transformed in the cortex into a whitish-

ash color due to the high concentration of small crescentic scars (e.g., artifacts such as 15A-P006-230812, 18AC-P065-311210, 7BJ-N001-201016 and 7AA-P056-050213 [20]).

On the sea beaches situated 50 km west of Pilauco, we have observed the existence of siliceous rocks other than glass with crescent marks ([20], Supplementary Figure S1). We think it is most likely that the volcanic glass clasts have collided with each other, because the fragility of this material would mean that if the collision was caused by a clast of another composition, density and texture, such as a basalt, the glass would break more easily. It is also possible to propose that the beaches where these surface marks would have originated may have been lake shore deposits, as occurs today in the Andes at this latitude where volcanoes and lakes intermingle. Lake beaches cannot exist in a glaciated environment. However, there is consensus that there was a rapid glacial retreat at this latitude of the Andes at the end of the Last Glacial Maximum [32]. This is also supported by seismic facies, sedimentological and diatom studies, which show an open lake, then beaches since at least 17,915 cal. Yr BP and possibly since ca. 24,750 cal. Yr BP [33–35].

In archaeology, experimentation has been used in many types of disciplines, from replication of use wear, zooarchaeology, taphonomy, pottery, to butchering experimentation [36–40]. In the field of transport experimentation, the contributions are very few, and rather refer to experiments in nature [41] or to the production of micro-traces by animal trampling, for example [42].

The principal aim of this experimental research is to study surface percussion marks and their production ratio on volcanic glass clasts, under a beach transport scenario. Additionally, the second objective is to compare the experimentally produced surface marks with the marks found in the cortex of archaeological samples.

3. Materials and Methods

Hundreds of obsidian clasts were collected in 2005 by MP from a large secondary obsidian deposit located along the southern shore of Laguna Blanca on the eastern slope of the Jarellón volcanic caldera, near the Chilean–Bolivian border [43] (Figure 1). The obsidian clasts had previously been described [44] as "small- to medium-sized, translucent black to reddish-brown, rounded pebbles from a secondary source and redeposited on the shores of a lake". The obsidian was heterogeneously distributed with variable densities between 500 and 1000 nodules m^{-2}, producing a uniform layer with soil development. Measured concentrations of incompatible elements such as Ba, Cs, Hf, Rb, Sr and Zr indicate that the samples correspond to alkaline or calcoalkaline obsidian [43,45].

One hundred obsidian clasts were used in this experiment. These had different sizes and shapes, well-rounded and polished edges, as well as a patina resulting from weathering in the Andes Altiplano, characterized as desert varnish. Of these clasts, 50 were used with their original shape (No. 101 to 150) and another 50 were intentionally fractured by direct percussion (No. 151 to 200). Each clast was identified with a number written in indelible black ink on a small white spot made with nail stain. Each of the 100 samples were repainted at the end of each experiment. The clasts were described considering the characteristics of surface marks and borders (e.g., smooth, rough, polished). The presence of indentations, grooves, striations, cracks and microfractures was also observed, as well as the type of luster present in the sample. The density of surface marks (feature cm^{-2}) and orientation (Figure 2), the presence of patinas and their color, rounding [46] and shape [47] were also measured. Photographs were taken of both sides of the clasts before and after each stage of the experiment using a Travor Softbox. Detailed photographs were also taken with a Leica S6D stereomicroscope and associated photographic equipment. Additionally, before and after each stage of experimental transport, length, width, thickness and mass were obtained for each clast. Lithic artifacts with a higher presence of cortex [9] were described and analyzed with the same parameters as the experimental artifacts. The description focused on the percussion crescent-shaped marks, their density and their orientation.
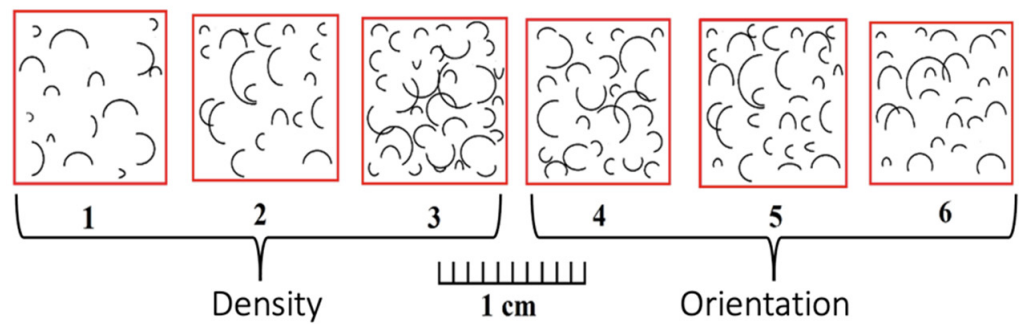
Figure 2. Graphical scheme used for the description of the density and orientation of surface marks 1 = <50 cm^{-2}, 2 = 50 to 100 cm^{-2}, 3 = >100 cm^{-2}, 4 = isotropic, 5 = intermediate, 6 = oriented.

The experimental work was carried out inside a wooden box 100 cm long, 60 cm wide and 10 cm high, half-filled with water. This box was connected to a three-phase motor type ML 7114, with 220 V and 1370 rpm. The equipment has a series of pulleys to decrease the angular velocity and a pulley with an eccentric connector to transform the rotary movement into an oscillating one. To facilitate the oscillating movement of the box (OB), it was mounted on wheels on rails. This OB was also divided into three equal parts (Supplementary Figure S2) whose separations allow the clasts to move mainly in the direction of the major axis of the OB, which favors the impact between them. The distance traveled, expressed as the duration of the experiments, was the only variable that determined the formation of microfractures or surface marks on the material being transported. As the box oscillates 21 cm forward and backward (total of 42 cm in one cycle), 78 cycles per minute, the clasts were moved 3276 cm min^{-1}. This last number was used to calculate the transport to which the clasts were subjected in the oscillating box. The samples were cleaned, and the surficial marks were analyzed at the end of each run. The same samples were used in the next transport experiment, until completing 20 km (Table 1). We used transport times of 21, 85, 170, 255, 340, 425 and 600 min (Table 1).

Table 1. Time and distance of transport in each experiment—both are cumulative.

	Experiment Number						
	1	**2**	**3**	**4**	**5**	**6**	**7**
Time (min)	21	85	170	255	340	425	600
Distance (km)	0.7	3	5.5	8.5	11	14	20

4. Results

The mean transport speed was 0.55 m s^{-1}. During the execution of the experiment, the clasts lost mass in the form of a fine, abrasive powder that leaves a record of a stippled surface below the major impact marks. The clasts fractured intentionally before the experiment had a higher mass loss (difference of 7%), a difference that is not significant (Table 2).

Table 2. Total mass loss after the experiment, for 50 natural and 50 intentionally broken clasts.

	Initial Mass (g)	**Final Mass (g)**	**Lost Mass (%)**
Natural clasts	1271	1209	5
Broken clasts	911	810	12

Figure 3 shows the half-moon (crescentic) surficial marks in a portion of the cortex of artifact 15B-P052-010316. More regular distribution of crescentic markings preserved in the cortex can be seen in artifact 15A-P006-230812, and the dark color of the vitreous dacite is observed in the incision in the lower part of Figure 4A. Here, crescent marks dominate with concentrations of ~100 cm^{-2} (Figure 4) [9,20].
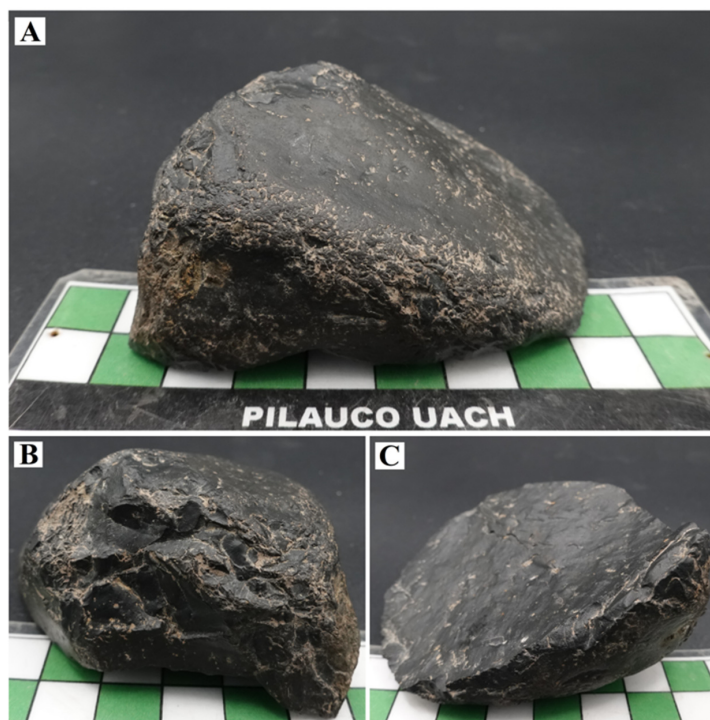

Figure 3. Artifact 15B-P052-010316. Pilauco site, layer PB-7. Typical black dacitic glass. The artifact corresponds to a thick flake from cobble, with an active convex-shaped distal edge, as well as part of the right side. The percussion point is on the left side of the ventral face (**C**). The crescentic marks are 0.2 to 1.5 mm long, and the marks are distributed irregularly only in the cortex (**A,B**). Each white and green square is 1 cm long.

Concerning the shape of the natural pebbles [27] (Figure 5), the samples were mainly classified as bladed (B, 46%), elongated (E, 10%), equidimensional bladed (CB, 10%) and very bladed (10%). As for the surface of the clasts, they had irregular surfaces, some smoothed indentations, as well as well-polished edges due to erosion. They also present desert patinas of a somewhat orange-brown color. Their L, I and S sizes ranged from 1.8 to 7.7 cm (mean 4.0 cm), 0.95 to 5 cm (mean 2.7 cm) and 0.95 to 2.6 cm (mean 1.6 cm), respectively. The mass varies between 2 to 91 g (mean 25 g). In the case of the set of fractured samples, these were presented the most in compact forms (C, 26%), then compact bladed (CB, 24%), compact elongate (CE, 10%), platy (*p*, 10%), bladed (B, 10%) and elongated (E, 10%). L-axes ranged from 1.7 to 4.7 cm (mean 3.9 cm), I-axes from 1.6 to 4 cm (mean 2.6 cm) and S-axes from 1 to 3.1 cm (mean 1.5 cm), with a mass ranging from 5 to 46 g (mean 24 g).

The clasts before the oscillatory transport experiment had three surface mark types and polished surfaces covered with desert patina. They are isolated or clustered crescentic marks of low density, and circular "craters" (Figure 6).

On the faces of the clasts during the experimental oscillatory transposition, four types of surface marks were originated and repeated both in the samples of natural form and those that were fractured. All types of marks have an isotropic orientation:

1. Crescent marks: They are characterized by having a crescent or half-moon shape, generally having clean edges and a vitreous luster characteristic of a conchoidal fracture. In the cobbles and pebbles without manipulation, they concentrate in a

greater density on the edges and faces with greater exposure. In the natural clasts, these marks measured from 2 to 9 mm long and had a density of up to 70 marks cm^{-2}. In the broken clast ensemble, the length was between 2 and 6 mm, also accumulating in greater quantity on the edges and freshly fractured faces (with greater exposure to collisions between clasts). They have a similar density of up to 65 marks cm^{-2} (Figures 7 and 8).

2. Circular marks: They correspond to a complete circle, easily distinguishable by their well-marked edges. They also have a vitreous luster characteristic of conchoidal fractures and stand out for the thickness of the edges, which are generally thicker than the crescent marks. Occasionally, two crescent marks may join to form a circular mark. Both in the natural and broken clasts, the length varies between 3 and 5 mm, and they have a low density comprising up to 5 marks cm^{-2} (Figures 7 and 8).

3. Pseudo-circular marks: The marks classified in this type are not perfectly circular in shape, with poorly defined edges, and in some cases are irregular. Most of them correspond to imperfect shapes with open ends, so in some cases they may resemble crescent marks. In the non-modified cobbles and pebbles, the length fluctuates between 2 and 8 mm, though these are very uncommon. In the broken clasts, these marks are between 2 and 15 mm long and can be observed associated with concave fractures, with well-marked circular edges and others with more irregular edges following a semi-circular shape (Figures 7 and 8). In addition, in this case, from 3 and up to 5 marks cm^{-2} were observed in the natural and broken sets, respectively.

4. Irregular marks: These marks do not follow a common pattern, nor do they have similar sizes, since they can range from millimetric to centimetric sizes. They are marks generated in thinner, weaker edges and therefore with a greater tendency to fracture. In the natural cobbles and pebbles, these marks do not follow a pattern and can be the largest, with lengths ranging from 2 to 14 mm. In the broken obsidian pieces, the length can vary from 1 to 12 mm (Figures 7 and 8). The concentration comprises up to 30 marks cm^{-2}.
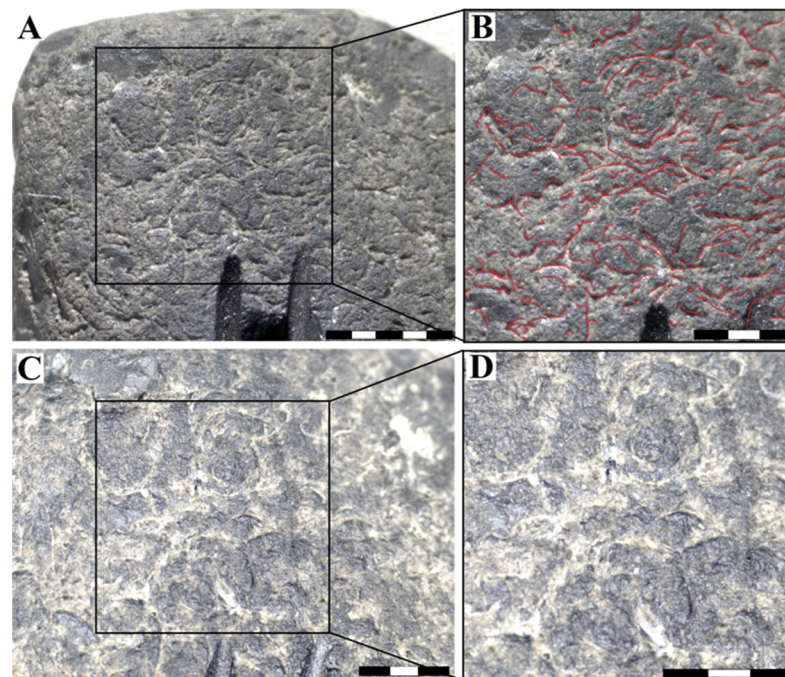

Figure 4. Details of the cortex of artifact 15-P0006-230812, knapped in dacitic glass. In the incision in the lower part of Figure 3A, the black color of the rock can be observed. (**A**,**B**) Normal photographs, and (**C**,**D**) stereomicroscope images. Each white and black rectangle is 1 mm long.
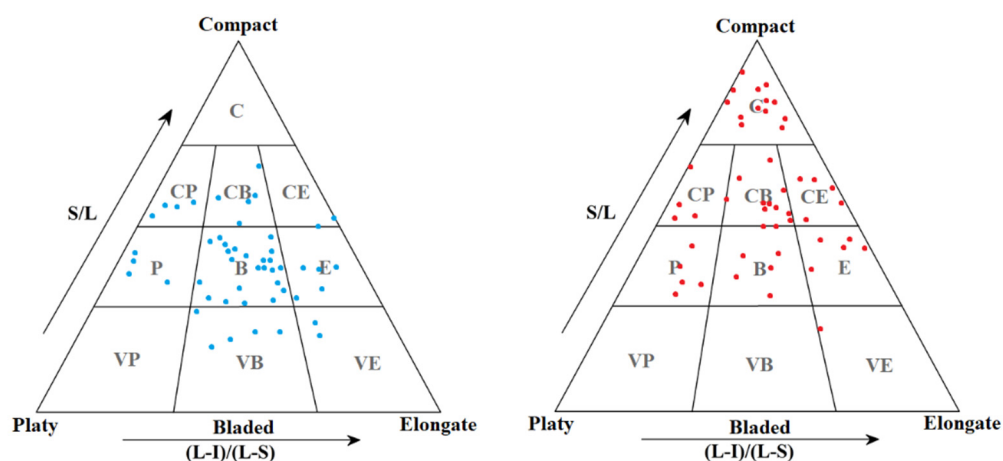
Figure 5. Clast shape classification diagram [27]. On the left, the light blue dots correspond to naturally shaped samples, and the red dots on the right represent artificially fractured samples. After breakage, the shapes became more compact.
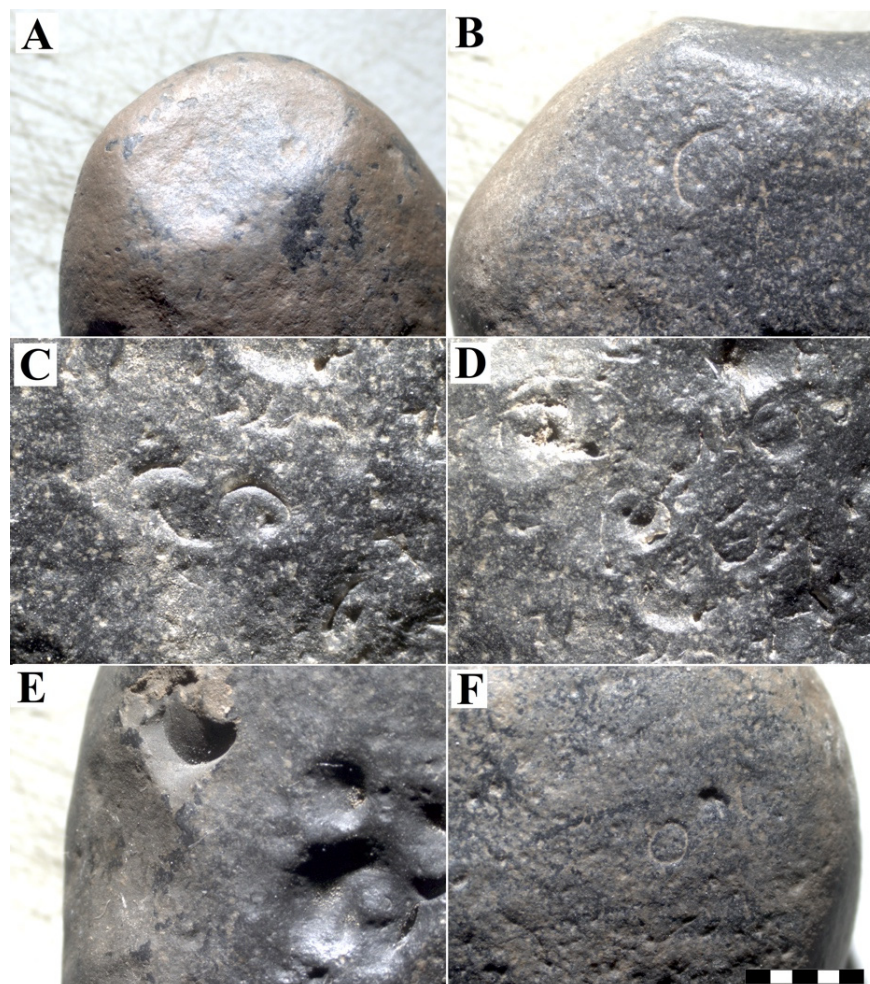

Figure 6. Main characteristics of the non-fractured natural samples prior to experimentation. Rounded, polished edges and a brownish desert patina (**A**,**B**), a rough surface with clustered crescentic marks (**C**,**D**) and rounded, clustered and isolated "crater" shaped notches (**E**,**F**) are visible. Isolated crescentic marks were also observed (**B**,**F**). The bottom right bar measures a total of 5 mm, the same from (**A–F**).
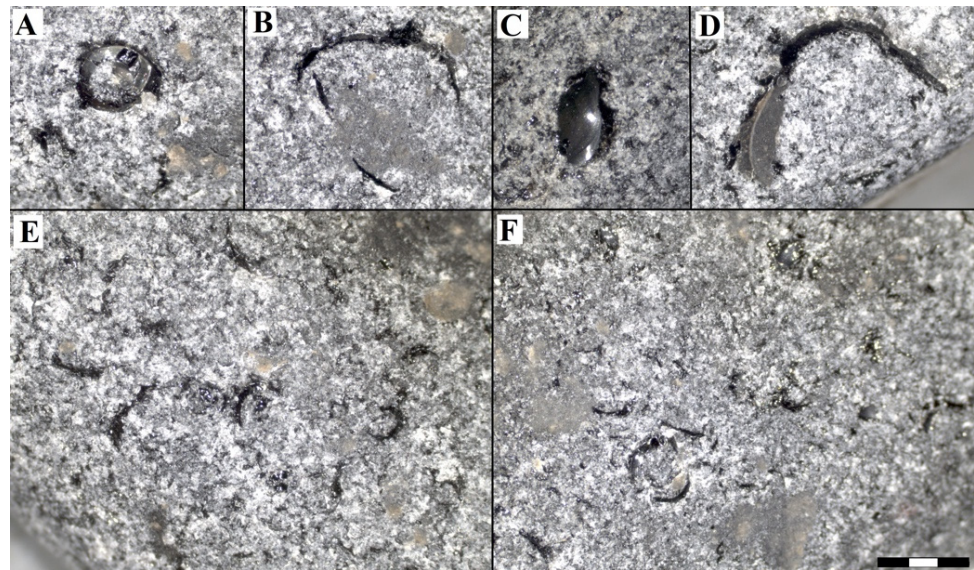
Figure 7. Different types of percussion marks generated in the experiment for the rounded samples: (**A**) circular, (**B**) crescent, (**C**) pseudo-circular, (**D–F**) crescent. The bottom right bar measures a total of 3 mm, the same from (**A–F**).

With respect to the density of the surface marks, Table 3 shows the maximum numbers achieved. The highest density was obtained in naturally shaped samples with a maximum of 70 marks cm^{-2}, a little higher than that observed in the set of fractured pieces (65 marks cm^{-2}), which was reached at the end of the experiment at 20 km of travel. The relationship between transport distance and mark density is statistically significant, because the *p*-value in the ANOVA table is less than 0.05 with a confidence level of 95.0%. The R-squared statistic indicates that the fitted model explains 97.1% of the variability in marks. The correlation coefficient is equal to 0.986, indicating a relatively strong relationship between the variables. The equation that relates both variables is:

$$mark\ density = 113.1859 + 146593\ \sqrt{transport}\ distance$$

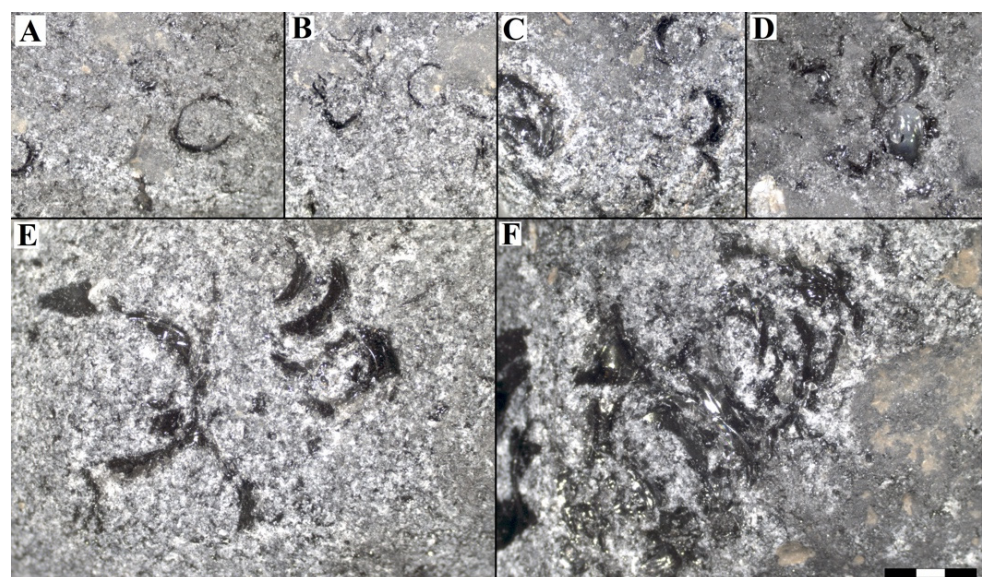**Figure 8.** Different types of percussion marks generated in the experiment for the broken samples: (**A–E**) crescent, (**C,D**) pseudo-circular, (**D**) circular, (**B–F**) irregular. The bottom right bar measures a total of 3 mm, the same from (**A–F**).

Table 3. Density ranges (marks cm^{-2}) in relation to the oscillatory transport distance separated into naturally shaped and intentionally broken clast assemblages.

	Transport Distance						
	0.7	**3**	**5.5**	**8.5**	**11**	**14**	**20**
Natural clasts	0–1	0–9	3–18	6–25	12–36	15–47	20–70
Broken clasts	0–3	0–10	5–22	8–29	12–37	15–42	19–65

That results indicate that the rate of percussion mark production was highest at the beginning of the experiment, up to 8.5 km, decreasing slightly thereafter. In relation to mass and patina loss, as an example, in sample 52, before the experiment the mass was 29 g and at the end of the 20 km of oscillatory transport it ended with 27 g, with a wear of 7%. The clast shows a 95% loss of the desert patina, conchoidal crescent and circular fractures up to 5 mm (Figures 9 and 10).
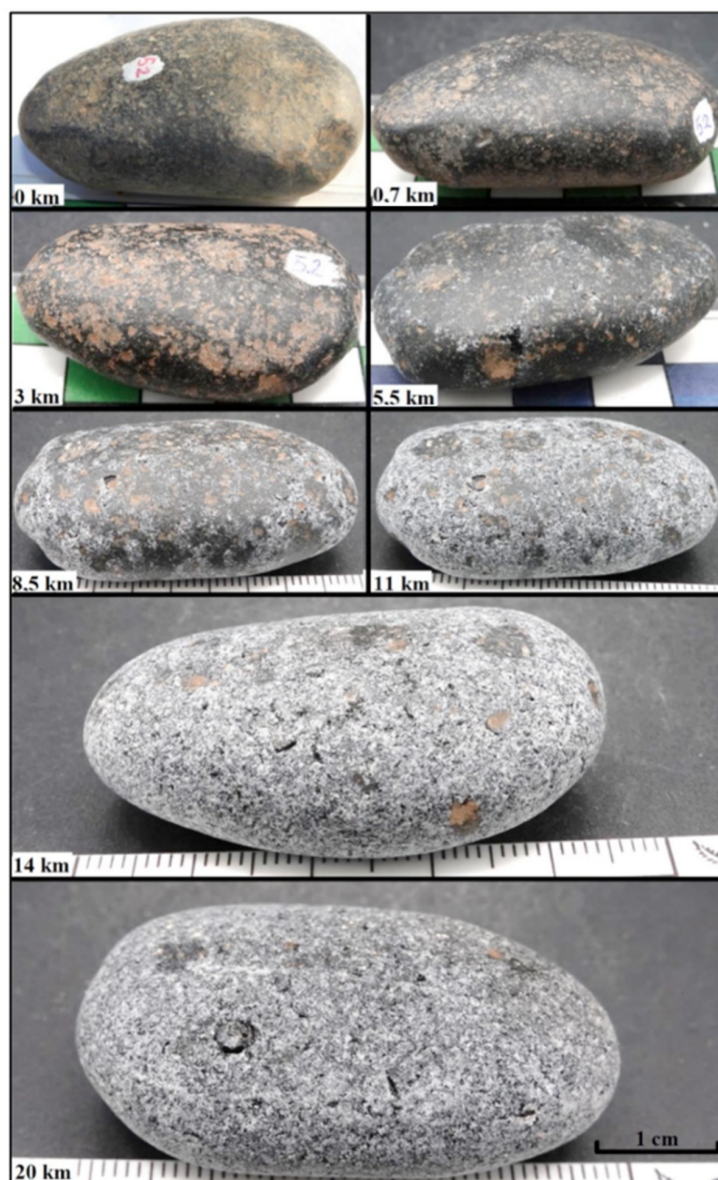

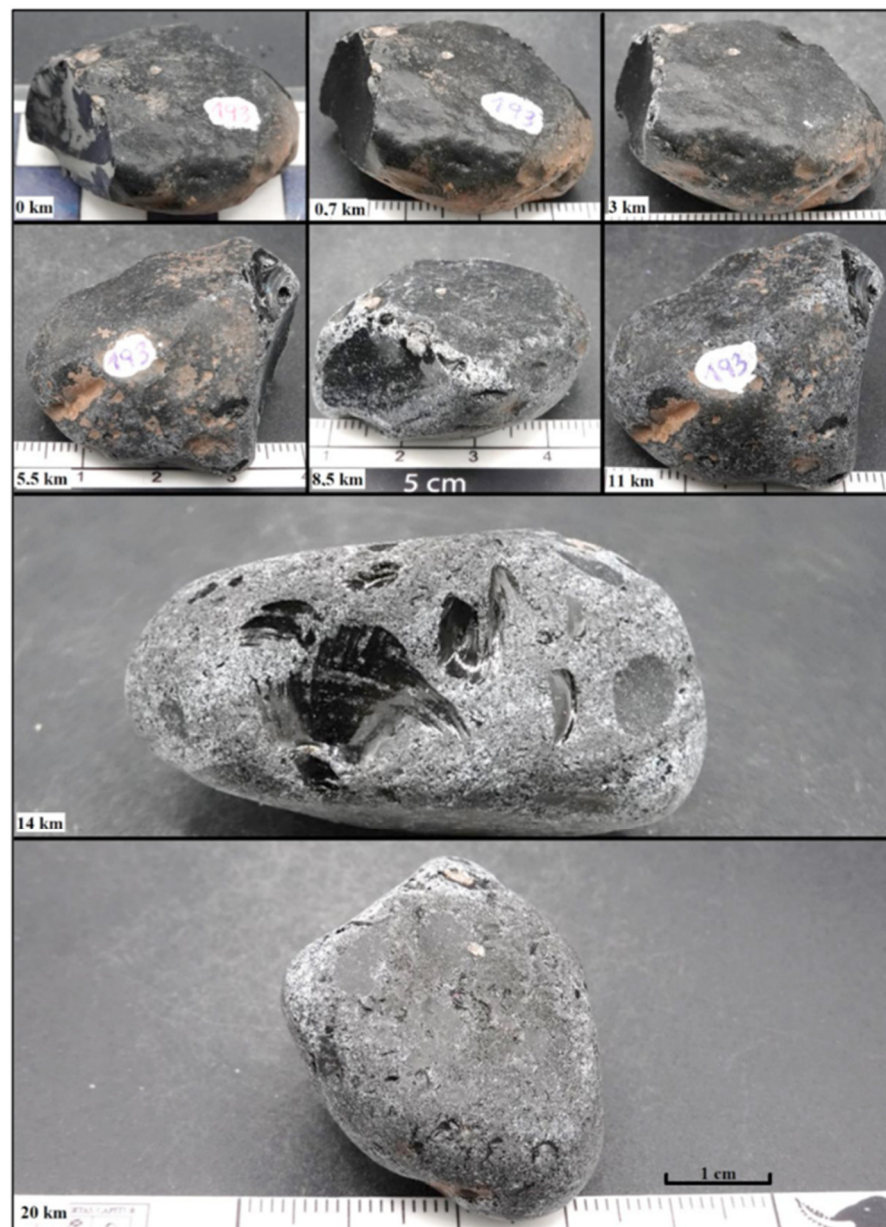**Figure 9.** Sample 52. Transport effects (from 0 to 20 km).

Figure 10. Sample 193, intentionally broken clast. Transport effects (from 0 to 20 km).

5. Discussion

The shapes described for the 3270 clasts collected in [43] in 2005 are concentrated (with great dispersion) within the compact bladed type, while the samples selected for this analysis presented a greater variety of shapes around the bladed group. This bias was probably produced by a series of selection and extraction processes of the obsidian collection for different educational and research purposes in Valdivia since 2005. Although the volcanic glasses used in this experiment correspond to obsidian [44] and the archaeological materials are dacitic glasses [9], it is very unlikely that the small differences in chemical composition (e.g., Ba and Zr concentrations [9]) between the two types of glasses originate any difference in the production of impact marks, regardless of the sedimentary environment. Some of the observed marks, such as the small "craters" (Figure 6E,F), were not described previously [43], and we think they could be vesicles opened during the experimental run. The other marks, clustered and isolated crescentic marks (Figure 6C,D), and the more frequent bladed shape of the obsidian clasts suggests that they acquired their shape and impact marks due to transport on the shores of a paleolake, thus recording

ancient higher levels of the present Laguna Blanca [43]. Given the previous last glacial maximum age of the obsidians, these cobbles and pebbles were transported a long time ago by a combination of first-order creek, snowmelt and gravity processes [43].

A detailed river transport experiment was carried out using a novel circular flume [47]. They used various lithologies, diameters from 10 to 80 mm and different speeds. They concluded that lithology controls both abrasion rates and abrasion processes, with differences in the former exceeding two orders of magnitude. Attrition, as well as breaking and splitting, are effective processes for reducing particle size. Mass loss by attrition increases with particle speed but has little dependence on particle size.

Our objective was to demonstrate that bidirectional transport could form surface marks similar to those observed in some dacitic volcanic glass artifacts at Pilauco. For this reason, our experiment was simpler than the one designed in [47], leaving speed and lithology constant. Additionally, there were no differences in weathering intensity and shapes in our clast collection [48,49]. The chosen average speed of 0.55 ms^{-1}, in the lower part of the speed range used in [47], did not cause breakage of the clasts, but had the capacity to obliterate the intentional fractures that were made in half of the clasts used in the experiment.

The attrition rate reported in [47] varied between ~0 and a maximum of 6% h^{-1}, depending on the amount of sediment mass and the diameter of the clasts. In our experiment, the attrition rate varied between 5% and 12% in 10 h, equivalent to 0.5% to 1.2% h^{-1}. This difference between mass loss using round and intentionally fractured clasts is however not statistically significant. It has been observed that the abrasion rate of angular clasts can be five times higher than the abrasion rate of rounded pebbles of similar diameter, due to edge abrasion, mainly by chipping [49,50], very different to our results.

6. Conclusions

We conclude that the novel transport device used here well-reproduces the bidirectional movement of clasts due to waves on a beach. The surface impact marks observed on the cortex of the dacitic glass artifacts recorded at the Pilauco site are similar to the ones developed in the first hours in our experimental flume. Thus, the archeological artifacts made of dacitic glass recorded at the Pilauco site suffered a minimum of 20 km of bidirectional transport distance. The angular clasts were rapidly rounded after a few kilometers of transport.

Conflicts of Interest: The authors declare no conflict of interest. The funders had no role in the design of the study; in the collection, analyses, or interpretation of data; in the writing of the manuscript, or in the decision to publish the results.

References

1. Anderson, D.G. Documenting early lithic technologies in South America. *Chungara* **2015**, *47*, 123–129. [CrossRef]
2. Dillehay, T.D. Entangled knowledge: Old trends and new thoughts in first South American studies. In *Paleoamerican Odyssey*; Graf, K.E., Ketron, C.V., Waters, M.R., Eds.; Texas A&M University Press: College Station, TX, USA, 2014; pp. 377–396, ISBN 978-1-62349-192-5.
3. Aceituno, F.J.; Loaiza, N.; Delgado-Burbano, M.E.; Barrientos, G. The initial human settlement of Northwest South America during the Pleistocene/Holocene transition: Synthesis and perspectives. *Quat. Int.* **2013**, *301*, 23–33. [CrossRef]
4. Brook, G.A.; Mancini, M.V.; Franco, N.V.; Bamonte, F.; Ambrústolo, P. An examination of possible relationships between paleoenvironmental conditions during the Pleistocene/Holocene transition and human occupation of southern Patagonia (Argentina) east of the Andes, between 46° and 52° S. *Quat. Int.* **2013**, *305*, 104–118. [CrossRef]
5. Dillehay, T.D. Monte Verde: A late Pleistocene Settlement in Chile. In *Paleoenvironmental and Site Context*; Smithsonian Institution Press: Washington, DC, USA, 1989. [CrossRef]
6. Dillehay, T.D. Monte Verde, a late Pleistocene Settlement in Chile. In *The Archaeological Context and Interpretation*; Smithsonian Institution Press: Washington, DC, USA, 1997. [CrossRef]
7. Pino, M.; Astorga, G. *Pilauco: A Late Pleistocene Archaeo-Paleontological Site. Osorno, Northwestern Patagonia and Chile*; Springer: Cham, Switzerland, 2020. [CrossRef]
8. Moreno, K.; Bostelmann, E.; Macías, C.; Navarro-Harris, X.; De Pol-Holz, R.; Pino, M. A late Pleistocene human footprint from the Pilauco archaeological site, Northern Patagonia, Chile. *PLoS ONE* **2019**, *14*, e0213572. [CrossRef] [PubMed]
9. Navarro-Harris, X.; Pino, M.; Guzmán-Marín, P.; Lira, M.P.; Labarca, R.; Corgne, A. The procurement and use of knappable glassy volcanic raw material, Upper Pleistocene Pilauco site, Chilean Northwestern Patagonia. *Geoarchaeology* **2019**, *34*, 592–612. [CrossRef]
10. Pino, M.; Chavez, M.; Navarro-Harris, X.; Labarca, R. The Late Pleistocene Pilauco Site, South Central Chile. *Quat. Int.* **2013**, *299*, 3–12. [CrossRef]
11. Pino, M.; Martel-Cea, A.; Vega, R.M.; Fritte, D.; Soto-Bollmann, K. Geology, Stratigraphy, and Chronology of the Pilauco Site. In *Pilauco: A Late Pleistocene Archaeo-Paleontological Site. Osorno, Northwestern Patagonia and Chile*; Pino, M., Astorga, G., Eds.; Springer: Cham, Switzerland, 2020; pp. 33–54. ISBN 978-3-030-23917-6. [CrossRef]
12. Pérez, A.; Navarro-Harris, X.; Boëda, E.; Pino, M. Beyond the mighty projectile point: Techno-functional study in a late Pleistocene artifact, Pilauco site, Osorno, northwestern Chilean Patagonia. *Lithic Technol.* **2021**. [CrossRef]
13. Borrero, L.; Franco, N.V. Early Patagonian Hunter-Gatherers: Subsistence and Technology. *J. Anthropol. Res.* **1997**, *53*, 219–239. [CrossRef]
14. Bryan, A.; Gruhn, R. Some difficulties in modeling the original peopling of the Americas. *Quat. Int.* **2003**, *109–110*, 175–179. [CrossRef]
15. Méndez, C.A.; Jackson, D. Terminal Pleistocene lithic technology and use of space in Central Chile. *Chungará* **2015**, *47*, 53–65. [CrossRef]
16. Giesso, M.; Berón, M.; Glascock, M. Obsidian in Western Pampas, Argentina: Source characterization and provisioning strategies. *APS Bull.* **2008**, *38*, 15–18.
17. Seelenfreund, A.; Fonseca, E.; Llona, F.; Lera, L.L.; Sinclaire, C.; Rees, C. Geochemical analysis of vitreous rocks exploited during the Formative period in the Atacama Region, northern Chile. *Archaeometry* **2009**, *51*, 1–25. [CrossRef]
18. Stern, C.R. Obsidian sources and distribution in Patagonia, southernmost South America. *Quat. Int.* **2018**, *468*, 190–205. [CrossRef]
19. Dillehay, T.D. *The Settlement of the Americas: A New Prehistory*; Basic Books: New York, NY, USA, 2000.
20. Navarro-Harris, X.; Pino, M.; Guzman-Marín, P. The Cultural Materials from Pilauco and Los Notros Sites. In *Pilauco: A Late Pleistocene Archaeo-Paleontological Site: Osorno, Northwestern Patagonia and Chile*; Pino, M., Astorga, G., Eds.; Springer: Cham, Switzerland, 2020; pp. 271–316. ISBN 978-3-030-23917-6. [CrossRef]
21. Borrero, L.A. Con lo mínimo: Los debates sobre el poblamiento de América del Sur. *Intersecc. Antropol.* **2015**, *16*, 5–38.
22. Roth, B.J. Obsidian source characterization and hunter–gatherer mobility: An example from the Tucson Basin. *J. Archaeol. Sci.* **2000**, *27*, 305–314. [CrossRef]
23. Stern, C.R.; Caracotche, S.; Cruz, I.; Charlin, J. Obsidiana gris porfírica calco-alcalina del volcán Chaitén en sitios arqueológicos al sur del río Santa Cruz, Patagonoa Meridional. *Magallania* **2012**, *40*, 135–142. [CrossRef]
24. Stern, C.R.; García, C.; Navarro-Harris, X.; Muñoz, J. Sources distribution of different types of obsidian from archaeological sites in central-south Chile (38–44° S). *Magallania* **2009**, *37*, 179–192. [CrossRef]
25. Stern, C.R.; Navarro-Harris, X.; Muñoz, J. Obsidiana gris translúcida del volcán Chaitén en los sitios arqueológicos de Quilo (Isla Grande Chiloé) y Chanchán (X Región), Chile, y obsidiana del Mioceno en Chiloé. *An. Inst. Patagon.* **2002**, *30*, 167–174.
26. Stern, C.R.; Navarro-Harris, X.; Pino, J.; Vega, R. Nueva fuente de obsidiana en la región de La Araucanía, centro sur de Chile: Química y contexto arqueológico de la obsidiana riolítica negra de los Nevados del Sollipulli. *Magallania* **2008**, *36*, 185–193. [CrossRef]

27. Vos, K.; Vandenberghe, N.; Elsen, J. Surface textural analysis of quartz grains by scanning electron microscopy (SEM): From sample preparation to environmental interpretation. *Earth-Sci. Rev.* **2014**, *128*, 93–104. [CrossRef]
28. Folk, R. *Petrology of Sedimentary Rocks*; Hemphill Pub.: Austin, TX, USA, 1980.
29. Wasson, R.J.; Sundriyal, Y.P.; Chaudhary, S.; Jaiswal, M.K.; Morthekai, P.; Sati, S.P.; Juyal, N. A 1000-year history of large floods in the Upper Ganga catchment, central Himalaya, India. *Quat. Sci. Rev.* **2013**, *77*, 156–166. [CrossRef]
30. de Vries Klein, G. Boulder Surface Markings in Quaco Formation (Upper Triassic), St. Martin's, New Brunswick, Canada. *J. Sediment. Res.* **1963**, *33*, 49–52. [CrossRef]
31. Krinsley, D.; Donahue, J. Pebble surface textures. *Geol. Mag.* **1968**, *105*, 521–525. [CrossRef]
32. McCulloch, R.D.; Bentley, M.J.; Purves, R.S.; Hulton, N.R.; Sugden, D.E.; Clapperton, C.M. Climatic inferences from glacial and paleoecological evidence at the last glacial termination, southern South America. *J. Quat. Sci.* **2000**, *15*, 409–417. [CrossRef]
33. Bertrand, S.; Charlet, F.; Charlier, B.; Renson, V.; Fagel, N. Climate variability of southern Chile since the Last Glacial Maximum: A continuous sedimentological record from Lago Puyehue (40°S). *J. Paleolimnol.* **2008**, *39*, 179–195. [CrossRef]
34. Charlet, F.; De Batist, M.; Chapron, E.; Bertrand, S.; Pino, M.; Urrutia, R. Seismic stratigraphy of Lago Puyehue (Chilean Lake District): New views on its deglacial and Holocene evolution. *J. Paleolimnol.* **2008**, *39*, 163–177. [CrossRef]
35. Sterken, M.; Verleyen, E.; Sabbe, K.; Terryn, G.; Charlet, F.; Bertrand, S.; Vyverman, W. Late Quaternary climatic changes in southern Chile, as recorded in a diatom sequence of Lago Puyehue (40 40′ S). *J. Paleolimnol.* **2008**, *39*, 219–235. [CrossRef]
36. Smith, K.N.; Vellanoweth, R.L.; Sholts, S.B.; Wärmländer, S.K. Residue analysis, use-wear patterns, and replicative studies indicate that sandstone tools were used as reamers when producing shell fishhooks on San Nicolas Island, California. *J. Archaeol. Sci. Rep.* **2018**, *20*, 502–505. [CrossRef]
37. Gilson, S.P.; St-Pierre, C.G.; Lominy, M.; Lessa, A. Shark teeth used as tools: An experimental archaeology study. *J. Archaeol. Sci. Rep.* **2021**, *35*, 102733. [CrossRef]
38. RufàBonache, A.; Alonso, G.; Blasco, R.; Cueto, M.; Camarós, E. Testing the damage caused by a golden eagle (Aquila chrysaetos) on a primate skull: A taphonomic case study of the bone damage observed after a simulated predatory attack. *Int. J. Osteoarchaeol.* **2020**, *30*, 789–797. [CrossRef]
39. Kudelić, A. Scientific-educational and popular program: Prehistoric pottery: Interdisciplinarity and experiment. *Ann. Inst. Archaeol.* **2019**, *15*, 233–238.
40. Starkovich, B.M.; Cuthbertson, P.; Kitagawa, K.; Thompson, N.; Konidaris, G.E.; Rots, V.; Münzel, S.C.; Giusti, D.; Schmid, V.C.; Blanco-Lapaz, A.; et al. Minimal Tools, Maximum Meat: A Pilot Experiment to Butcher an Elephant Foot and Make Elephant Bone Tools Using Lower Paleolithic Stone Tool Technology. *Ethnoarchaeology* **2020**, *12*, 118–147. [CrossRef]
41. Chu, W.; Hosfield, R. Lithic artifact assemblage transport and microwear modification in a fluvial setting: A radio frequency identification tag experiment. *Geoarchaeology* **2020**, *35*, 591–608. [CrossRef]
42. Schoville, B.J. Experimental lithic tool displacement due to long-term animal disturbance. *Archaeol. Anthropol. Sci.* **2019**, *11*, 5879–5891. [CrossRef]
43. Seelenfreund, A.; Pino, M.; Glascock, M.D.; Sinclaire, C.; Miranda, P.; Pasten, D.; Cancino, S.; Dinator, M.I.; Morales, J.R. Morphological and geochemical analysis of the Laguna Blanca/Zapaleri obsidian source in the Atacama Puna. *Geoarchaeology* **2010**, *25*, 245–263. [CrossRef]
44. Nielsen, A.; Vázquez, M.; Avalos, J.; Angiorama, C. Prospecciones arqueológicas en la reserva "Eduardo Abaroa" (Sud Lípez, Depto. Potosí, Bolivia). *Textos Antropológicos* **2000**, *11*, 89–131.
45. Shackley, S. *Obsidian: Geology and Archaeology in the North American Southwest*; University of Arizona Press: Tucson, AZ, USA, 2005.
46. Powers, M.C. *Comparison Chart for Estimating Roundness and Sphericity: AGI*; American Geological Institute: Alexandria, VA, USA, 1982; Data Sheet 18.1.
47. Attal, M.; Lavé, J. Pebble abrasion during fluvial transport: Experimental results and implications for the evolution of the sediment load along rivers. *J. Geophys. Res. Earth Surf.* **2009**, *114*. [CrossRef]
48. Krumbein, W.C. The effects of abrasion on the size, shape and roundness of rock fragments. *J. Geol.* **1941**, *49*, 482–520. [CrossRef]
49. Kuenen, P.H. Experimental erosion of pebbles: 2. Rolling by current. *J. Geol.* **1956**, *64*, 336–368. [CrossRef]
50. Lewin, J.; Brewer, P.A. Laboratory simulation of clast abrasion. *Earth Surf. Process. Landf.* **2002**, *27*, 145–164. [CrossRef]